Probing BFKL resummation at hadronic colliders

Christophe Royon [e, i, j]

[e]The University of Kansas, Lawrence, USA

[i]Institute of Physics, Academy of Science of the Czech Republic, Prague, Czech Republic

[j]Institute of Nuclear Physics, Polish Academy of Sciences, Krakow, Poland

Abstract

We describe two different possible measurements sensitive to BFKL resummation effects to be performed at the LHC, namely the Mueller Navelet jets and the jet gap jet cross sections. We perform a NLL calculation of these processes and compare it to recent Tevatron measurements, and give predictions at LHC energies. We also discuss the possibility of measuring jet gap jet events in diffraction at the LHC.

1 Mueller Navelet jets at the LHC

In this section, we give the BFKL NLL cross section calculation for Mueller Navelet processes at the Tevatron and the LHC. Since the starting point of this study was the description of forward jet production at HERA, we start by describing briefly these processes.

1.1 Forward jets at HERA

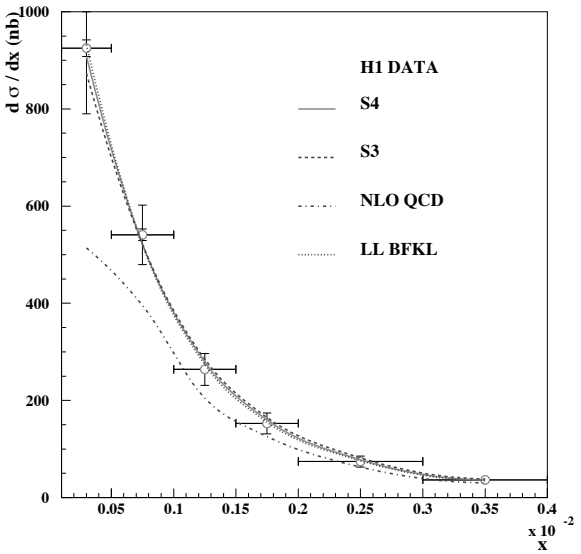

Figure 135: Comparison between the H1 $d\sigma/dx$ measurement with predictions for BFKL-LL, BFKL-NLL (S3 and S4 schemes) and DGLAP NLO calculations (see text). S4, S3 and LL BFKL cannot be distinguished on that figure.

Following the successful BFKL [1] parametrisation of the forward-jet cross-section $d\sigma/dx$ at Leading Order (LO) at HERA [2, 3], it is possible to perform a similar study using Next-to-leading (NLL) resummed BFKL kernels. Forward jets at HERA are an ideal observable to look for BFKL resummation effects. The interval in rapidity between the scattered lepton and the jet in the forward region is large,

and when the photon virtuality Q is close to the transverse jet momentum k_T, the DGLAP cross section is small because of the k_T ordering of the emitted gluons. In this short report, we will only discuss the phenomelogical aspects and all detailed calculations can be found in Ref. [4] for forward jets at HERA and in Ref. [5] for Mueller Navelet jets at the Tevatron and the LHC.

1.2 BFKL NLL formalism

The BFKL NLL [6] longitudinal transverse cross section reads:

$$\frac{d\sigma_{T,L}^{\gamma^* p \to JX}}{dx_J dk_T^2} = \frac{\alpha_s(k_T^2)\alpha_s(Q^2)}{k_T^2 Q^2}\ f_{eff}(x_J, k_T^2) \int d\gamma \left(\frac{Q^2}{k_T^2}\right)^{\gamma} \phi_{T,L}^{\gamma}(\gamma)\ e^{\bar{\alpha}\chi_{eff}Y} \tag{359}$$

where x_J is the proton momentum fraction carried by the forward jet, χ_{eff} is the effective BFKL NLL kernel and the ϕs are the transverse and longitunal impact factors taken at LL. The effective kernel $\chi_{eff}(\gamma, \bar{\alpha})$ is defined from the NLL kernel $\chi_{NLL}(\gamma, \omega)$ by solving the implicit equation numerically

$$\chi_{eff}(\gamma, \bar{\alpha}) = \chi_{NLL}\left[\gamma, \bar{\alpha}\ \chi_{eff}(\gamma, \bar{\alpha})\right]\ . \tag{360}$$

The integration over γ in Eq. 359 is performed numerically. It is possible to fit directly $d\sigma/dx$ measured by the H1 collaboration using this formalism with one single parameter, the normalisation. The values of χ_{NLL} are taken at NLL [6] using different resummation schemes to remove spurious singularities defined as S3 and S4 [7]. Contrary to LL BFKL, it is worth noticing that the coupling constant α_S is taken using the renormalisation group equations, the only free parameter in the fit being the normalisation.

To compute $d\sigma/dx$ in the experimental bins, we need to integrate the differential cross section on the bin size in Q^2, x_J (the momentum fraction of the proton carried by the forward jet), k_T , while taking into account the experimental cuts. To simplify the numerical calculation, we perform the integration on the bin using the variables where the cross section does not change rapidly, namely k_T^2/Q^2, $\log 1/x_J$, and $1/Q^2$. Experimental cuts are treated directly at the integral level (the cut on $0.5 < k_T^2/Q^2 < 5$ for instance) or using a toy Monte Carlo. More detail can be found about the fitting procedure in Appendix A of Ref. [3].

The NLL fits [4] can nicely describe the H1 data [8] for the S4 and S3 schemes [2–4] ($\chi^2 = 0.48/5$ and $\chi^2 = 1.15/5$ respectively per degree of freedom with statistical and systematic errors added in quadrature). The curve using a LL fit is indistinguishable in Fig. 135 from the result of the BFKL-NLL fit. The DGLAP NLO calculation fails to describe the H1 data at lowest x (see Fig. 135). We also checked the effect of changing the scale in the exponential of Eq. 359 from $k_T Q$ to $2k_T Q$ or $k_T Q/2$ which leads to a difference of 20% on the cross section while changing the scale to k_T^2 or Q^2 modifies the result by less than 5% which is due to the cut on $0.5 < k_T^2/Q^2 < 5$. Implementing the higher-order corrections in the impact factor due to exact gluon dynamics in the $\gamma^* \to q\bar{q}$ transition [9] changes the result by less than 3%.

The H1 collaboration also measured the forward jet triple differential cross section [8] and the results are given in Fig. 136. We keep the same normalisation coming from the fit to $d\sigma/dx$ to predict the triple differential cross section. The BFKL LL formalism leads to a good description of the data when $r = k_T^2/Q^2$ is close to 1 and deviates from the data when r is further away from 1. This effect is expected since DGLAP radiation effects are supposed to occur when the ratio between the jet k_T and the virtual photon Q^2 are further away from 1. The BFKL NLL calculation including the Q^2 evolution via the renormalisation group equation leads to a good description of the H1 data on the full range. We note that the higher order corrections are small when $r \sim 1$, when the BFKL effects are supposed to dominate. By contrast, they are significant as expected when r is different from one, ie when DGLAP evolution becomes relevant. We notice that the DGLAP NLO calculation fails to describe the data when $r \sim 1$, or in the region where BFKL resummation effects are expected to appear.

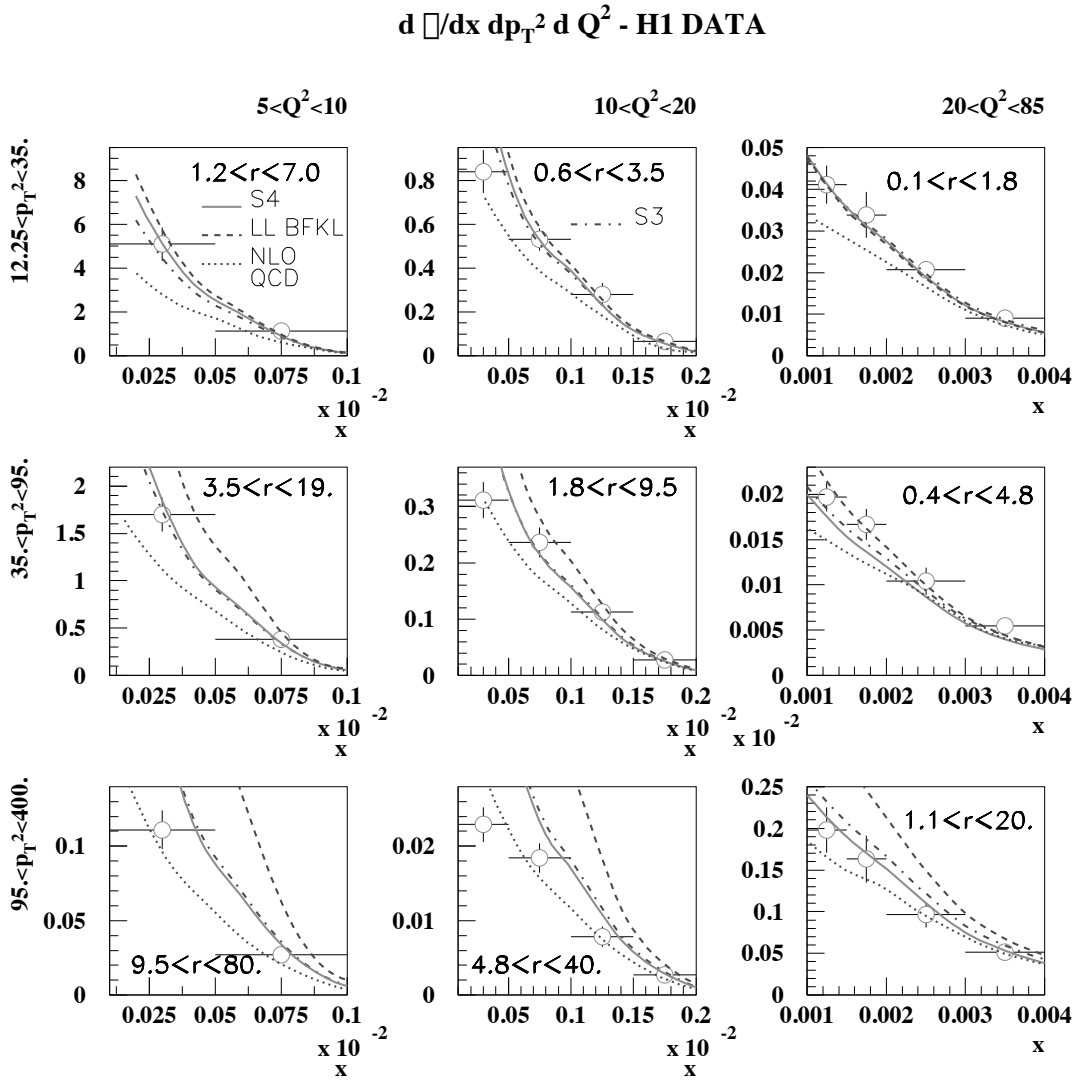

Figure 136: Comparison between the H1 measurement of the triple differential cross section with predictions for BFKL-LL, BFKL-NLL and DGLAP NLO calculations (see text).

In addition, we checked the dependence of our results on the scale taken in the exponential of Eq. 359. The effect is a change of the cross section of about 20% at low p_T increasing to 70% at highest p_T. Taking the correct gluon kinematics in the impact factor lead as expected to a better description of the data at high p_T [4].

1.3 Mueller Navelet jets at the Tevatron and the LHC

Mueller Navelet jets are ideal processes to study BFKL resummation effects [5]. Two jets with a large interval in rapidity and with similar tranverse momenta are considered. A typical observable to look for BFKL effects is the measurement of the azimuthal correlations between both jets. The DGLAP prediction is that this distribution should peak towards π - ie jets are back-to-back- whereas multi-gluon emission via the BFKL mechanism leads to a smoother distribution. The relevant variables to

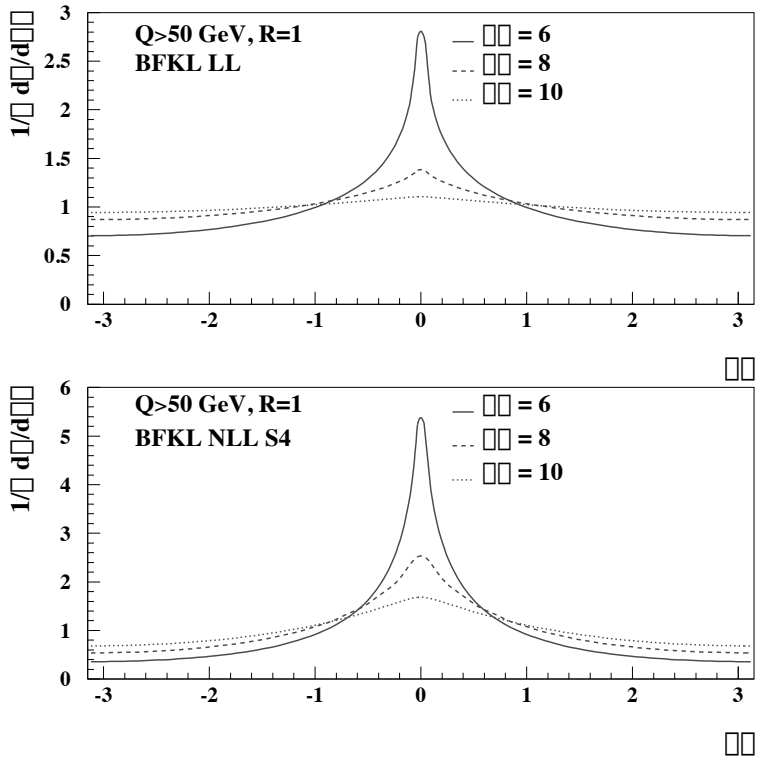

Figure 137: The Mueller-Navelet jet $\Delta\Phi$ distribution for LHC kinematics in the BFKL framework at LL (upper plots) and NLL-S4 (lower plots) accuracy for $\Delta\eta = 6,\ 8,\ 10$.

look for azimuthal correlations are the following:

$$\begin{aligned} \Delta\eta &= y_1 - y_2 \\ y &= (y_1 + y_2)/2 \\ Q &= \sqrt{k_1 k_2} \\ R &= k_2/k_1 \end{aligned}$$

where $y_{1,2}$ and $k_{1,2}$ are respectively the jet rapidities and transverse momenta. The azimuthal correlation for BFKL reads:

$$2\pi \frac{d\sigma}{d\Delta\eta dR d\Delta\Phi} \Big/ \frac{d\sigma}{d\Delta\eta dR} = 1 + \frac{2}{\sigma_0(\Delta\eta, R)} \sum_{p=1}^{\infty} \sigma_p(\Delta\eta, R) \cos(p\Delta\Phi)$$

where in the NLL BFKL framework,

$$\begin{aligned} \sigma_p &= \int_{E_T}^{\infty} \frac{dQ}{Q^3} \alpha_s(Q^2/R)\alpha_s(Q^2R) \left(\int_{y_<}^{y_>} dy x_1 f_{eff}(x_1, Q^2/R) x_2 f_{eff}(x_2, Q^2R) \right) \\ & \int_{1/2-\infty}^{1/2+\infty} \frac{d\gamma}{2i\pi} R^{-2\gamma}\ e^{\bar{\alpha}(Q^2)\chi_{eff}(p,\gamma,\bar{\alpha})\Delta\eta} \end{aligned}$$

and χ_{eff} is the effective resummed kernel. Computing the different σ_p at NLL for the resummation schemes S3 and S4 allowed us to compute the azimuthal correlations at NLL. As expected, the $\Delta\Phi$ dependence is less flat than for BFKL LL and is closer to the DGLAP behaviour [5]. In Fig. 137, we display the observable $1/\sigma d\sigma/d\Delta\Phi$ as a function of $\Delta\Phi$, for LHC kinematics. The results are displayed for different values of $\Delta\eta$ and at both LL and NLL accuracy using the S4 resummation

scheme. In general, the $\Delta\Phi$ spectra are peaked around $\Delta\Phi = 0$, which is indicative of jet emissions occuring back-to-back. In addition the $\Delta\Phi$ distribution flattens with increasing $\Delta\eta = y_1 - y_2$. Note the change of scale on the vertical axis which indicates the magnitude of the NLL corrections with respect to the LL-BFKL results. The NLL corrections slow down the azimuthal angle decorrelations for both increasing $\Delta\eta$ and R deviating from 1. We also studied the R dependence of our prediction which is quite weak [5] and the scale dependence of our results by modifying the scale Q^2 to either $Q^2/2$ or $2Q^2$ and the effect on the azimuthal distribution is of the order of 20%. The effect of the energy conservation in the BFKL equation [5] is large when R goes away from 1. The effect is to reduce the effective value of $\Delta\eta$ between the jets and thus the decorrelation effect. However, it is worth noticing that this effect is negligible when R is close to 1 where this measurement will be performed. Recent calculations include in addition NLL impact factors [5].

A measurement of the cross-section $d\sigma^{hh\mapsto JXJ}/d\Delta\eta dR d\Delta\Phi$ at the LHC will allow for a detailed study of the BFKL QCD dynamics since the DGLAP evolution leads to much less jet angular decorrelation (jets are back-to-back when R is close to 1). In particular, measurements with values of $\Delta\eta$ reaching 8 or 10 using the CASTOR calorimeter of the CMS collaboration for instance will be of great interest, as these could allow to distinguish between BFKL and DGLAP resummation effects and would provide important tests for the relevance of the BFKL formalism.

2 Jet veto measurements in ATLAS

The ATLAS collaboration measured the so-called jet veto cross section [10], namely the events with two high p_T jets, well separated in rapidity and with a veto on jet activity with p_T greater than a given threshold Q_0 between the two jets. The ATLAS collaboration measured the jet veto fraction with respect to the standard dijet cross section, and it was advocated that it might be sensitive to BFKL dynamics. In Ref. [11], we computed the gluon emission at large angles (which are not considered in usual MC) using the Banfi-Marchesini-Smye equation, and we showed that the measurement can be effectively described by the gluon resummation and is thus not related to BFKL dynamics as shown in Fig. 138. The sensivity to the BFKL resummation effects appears when one looks for gaps between jets as described in the following section.

3 Jet gap jets at the Tevatron and the LHC

In this section, we describe another possible measurement which can probe BFKL resummation effects and we compare our predictions with existing D0 and CDF measurements [12].

3.1 BFKL NLL formalism

The production cross section of two jets with a gap in rapidity between them reads

$$\frac{d\sigma^{pp\to XJJY}}{dx_1 dx_2 dE_T^2} = \mathcal{S} f_{eff}(x_1, E_T^2) f_{eff}(x_2, E_T^2) \frac{d\sigma^{gg\to gg}}{dE_T^2}, \tag{361}$$

where $\sqrt{s}$ is the total energy of the collision, E_T the transverse momentum of the two jets, x_1 and x_2 their longitudinal fraction of momentum with respect to the incident hadrons, S the survival probability, and f the effective parton density functions [12]. The rapidity gap between the two jets is $\Delta\eta = \ln(x_1 x_2 s/p_T^2)$.

The cross section is given by

$$\frac{d\sigma^{gg\to gg}}{dE_T^2} = \frac{1}{16\pi} \left| A(\Delta\eta, E_T^2) \right|^2 \tag{362}$$

in terms of the $gg \to gg$ scattering amplitude $A(\Delta\eta, p_T^2)$.

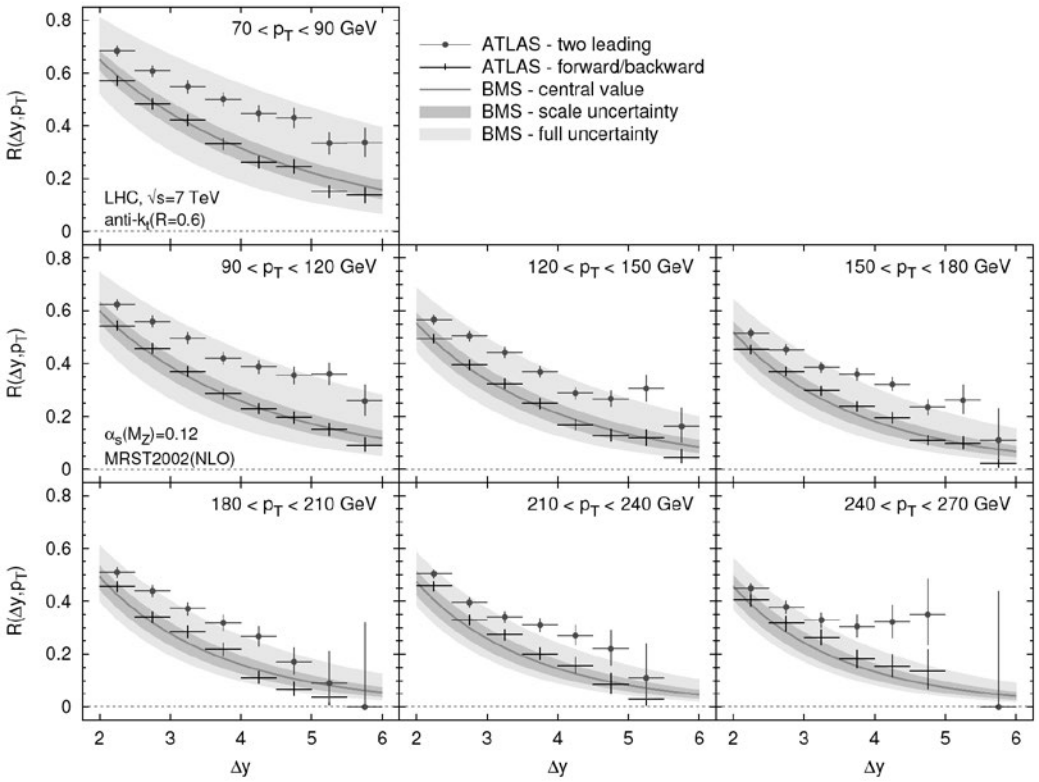

Figure 138: Comparison of the resummed veto fraction with the ATLAS measurement, for a fixed veto energy of $E_{out} = 20$ GeV, in different bins of p_T . The inner (green) uncertainty band is obtained taking into account only the renormalization and factorization scale uncertainties, while the outer (yellow) band also includes the subleading logarithmic uncertainty. For the ATLAS data, circles represent the case where the two leading jets are selected while the one where the most forward and backward jets are selected are represented by crosses.

In the following, we consider the high energy limit in which the rapidity gap $\Delta\eta$ is assumed to be very large. The BFKL framework allows to compute the $gg \to gg$ amplitude in this regime, and the result is known up to NLL accuracy

$$A(\Delta\eta, E_T^2) = \frac{16 N_c \pi \alpha_s^2}{C_F E_T^2} \sum_{p=-\infty}^{\infty} \int \frac{d\gamma}{2i\pi} \frac{[p^2 - (\gamma - 1/2)^2]}{[(\gamma - 1/2)^2 - (p - 1/2)^2]} \frac{\exp\left\{\bar{\alpha}(E_T^2)\chi_{eff}[2p, \gamma, \bar{\alpha}(E_T^2)]\Delta\eta\right\}}{[(\gamma - 1/2)^2 - (p + 1/2)^2]} \tag{363}$$

with the complex integral running along the imaginary axis from $1/2 - i\infty$ to $1/2 + i\infty$, and with only even conformal spins contributing to the sum, and $\bar{\alpha} = \alpha_S N_C/\pi$ the running coupling.

As for the Mueller-Navelet jets, the NLL-BFKL effects are phenomenologically taken into account by the effective kernels $\chi_{eff}(p, \gamma, \bar{\alpha})$. The NLL kernels obey a *consistency condition* which allows to reformulate the problem in terms of $\chi_{eff}(\gamma, \bar{\alpha})$.

In this study, we performed a parametrised distribution of $d\sigma^{gg\to gg}/dE_T^2$ so that it can be easily implemented in the Herwig Monte Carlo [13] since performing the integral over γ in particular would be too much time consuming in a Monte Carlo. The implementation of the BFKL cross section in a Monte Carlo is absolutely necessary to make a direct comparison with data. Namely, the measurements are sensititive to the jet size (for instance, experimentally the gap size is different from the rapidity interval between the jets which is not the case by definition in the analytic calculation).

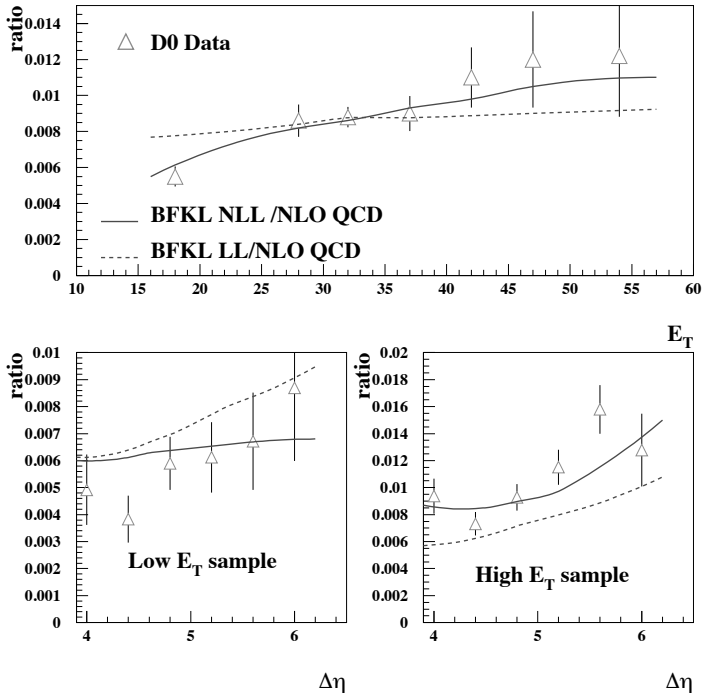

Figure 139: Comparisons between the D0 measurements of the jet-gap-jet event ratio with the NLL- and LL-BFKL calculations. The NLL calculation is in fair agreement with the data. The LL calculation leads to a worse description of the data.

3.2 Comparison with D0 and CDF measurements

Let us first notice that the sum over all conformal spins is absolutely necessary. Considering only $p = 0$ in the sum of Equation 363 leads to a wrong normalisation and a wrong jet E_T dependence, and the effect is more pronounced as $\Delta\eta$ diminishes.

The D0 collaboration measured the jet gap jet cross section ratio with respect to the total dijet cross section, requesting for a gap between -1 and 1 in rapidity, as a function of the second leading jet E_T, and $\Delta\eta$ between the two leading jets for two different low and high E_T samples (15< E_T <20 GeV and E_T >30 GeV). To compare with theory, we compute the following quantity

$$Ratio = \frac{BFKL\ NLL\ HERWIG}{Dijet\ Herwig} \times \frac{LO\ QCD}{NLO\ QCD} \tag{364}$$

in order to take into account the NLO corrections on the dijet cross sections, where $BFKL\ NLL\ HERWIG$ and $Dijet\ Herwig$ denote the BFKL NLL and the dijet cross section implemented in HERWIG. The NLO QCD cross section was computed using the NLOJet++ program [14].

The comparison with D0 data [15] is shown in Fig. 139. We find a good agreement between the data and the BFKL calculation. It is worth noticing that the BFKL NLL calculation leads to a better result than the BFKL LL one (note that most studies in the literature considered only the $p = 0$ component which is not a valid assumption).

The comparison with the CDF data [15] as a function of the average jet E_T and the difference in rapidity between the two jets is shown in Fig. 140, and the conclusion remains the same: the BFKL NLL formalism leads to a better description than the BFKL LL one.

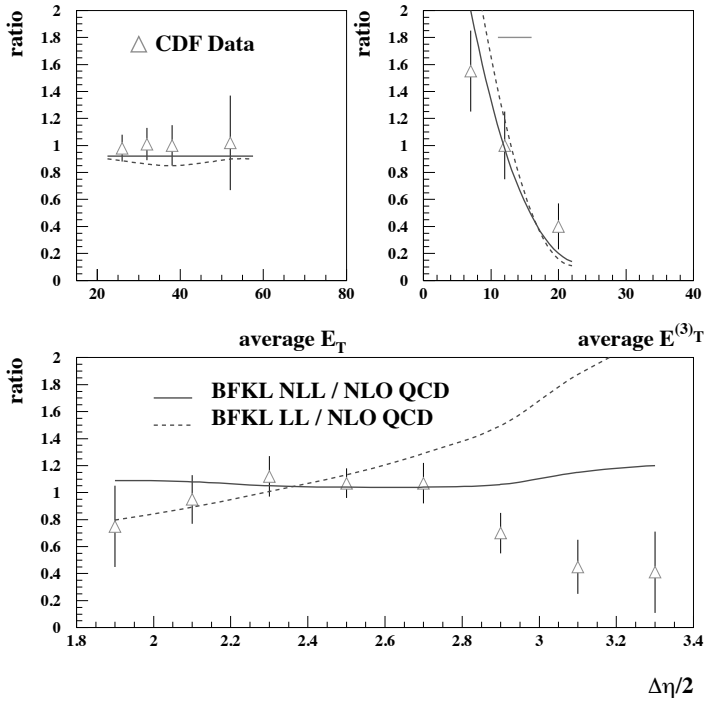

Figure 140: Comparisons between the CDF measurements of the jet-gap-jet event ratio with the NLL- and LL-BFKL calculations. The NLL calculation is in fair agreement with the data. The LL calculation leads to a worse description of the data.

3.3 Predictions for the LHC

Using the same formalism, and assuming a survival probability of 0.03 at the LHC, it is possible to predict the jet gap jet cross section at the LHC. While both LL and NLL BFKL formalisms lead to a weak jet E_T or $\Delta\eta$ dependence, the normalisation is found to be quite different (see Fig. 141) leading to lower cross section for the BFKL NLL formalism.

4 Jet gap jet events in diffraction at the LHC

A new process of detecting jet-gap-jet events in diffractive double pomeron exchange processes was introduced recently [16]. The idea is to tag the intact protons inside the ATLAS Forward Physics (AFP) detectors [17] located at about 210 m from the ATLAS interaction point on both sides. The advantage of such processes is that they are quite clean since they are not "polluted" by proton remnants and it is possible to go to larger jet separation than for usual jet-gap-jet events. The normalisation for these processes come from the fit to the D0 discussed in the previous section. The ratio between jet-gap-jet to inclusive jet events is shown in Fig. 142 requesting protons to be tagged in AFP for both samples. The ratio shows a weak dependence as a function of jet p_T (and also as a function of the difference in rapidity between the two jets). It is worth noticing that the ratio is about 20-30% showing that the jet-gap-jet events are much more present in the diffractive sample than in the inclusive one as expected.

It is worth noticing that there are many measurements that can be performed in diffraction in addition to the search for BFKL dymamics in jet gap jet events [18]

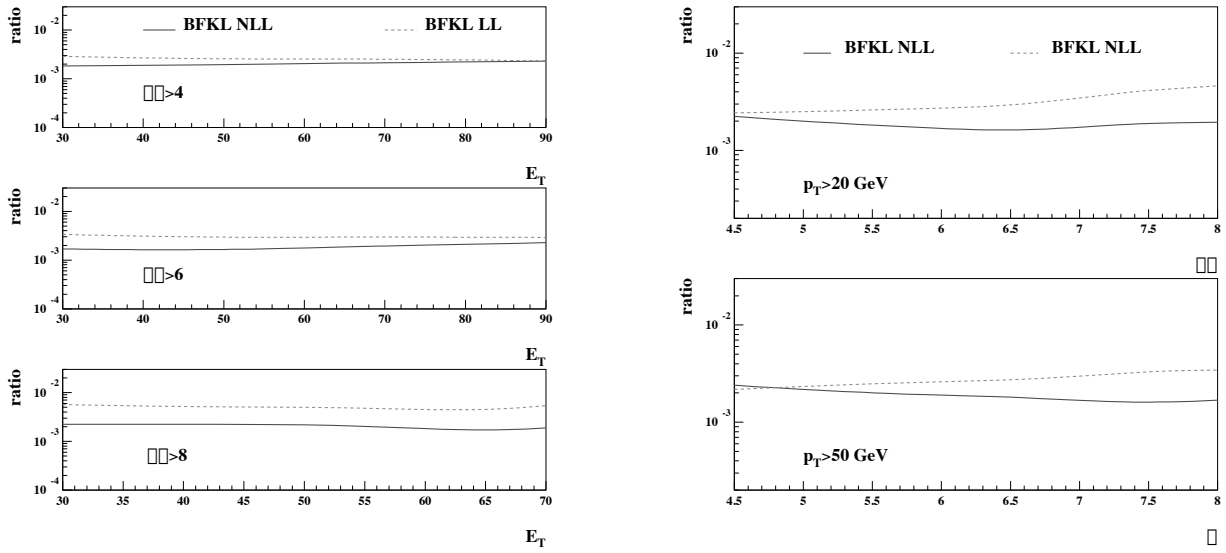

Figure 141: Ratio of the jet gap jet to the inclusive jet cross sections at the LHC as a function of jet p_T and $\Delta\eta$.

5 Conclusion

In this short paper, we presented different observables sensitive to BFKL dynamics that can be looked at especially at the LHC, namely the Mueller Navelet jets and the gap between jets in standard or diffractive events. Some mew measurements are expected soon and might lead to a clear signature.

References

1. L. N. Lipatov, Sov. J. Nucl. Phys. **23**, 338 (1976) [Yad. Fiz. **23**, 642 (1976)]; E. A. Kuraev, L. N. Lipatov and V. S. Fadin, Sov. Phys. JETP **45**, 199 (1977) [Zh. Eksp. Teor. Fiz. **72**, 377 (1977)]; I. I. Balitsky and L. N. Lipatov, Sov. J. Nucl. Phys. **28**, 822 (1978) [Yad. Fiz. **28**, 1597 (1978)].
2. J. G. Contreras, R. B. Peschanski and C. Royon, Phys. Rev. D **62**, 034006 (2000) [hep-ph/0002057 [hep-ph]]; C. Marquet, R. B. Peschanski and C. Royon, Phys. Lett. B **599**, 236 (2004) [hep-ph/0407011 [hep-ph]].
3. C. Marquet and C. Royon, Nucl. Phys. B **739**, 131 (2006) [hep-ph/0510266 [hep-ph]].
4. O. Kepka, C. Royon, C. Marquet and R. B. Peschanski, Phys. Lett. B **655**, 236 (2007) [hep-ph/0609299 [hep-ph]]; O. Kepka, C. Royon, C. Marquet and R. B. Peschanski, Eur. Phys. J. C **55**, 259 (2008) [hep-ph/0612261 [hep-ph]]; C. Marquet and C. Royon, Phys. Rev. D **79**, 034028 (2009) [arXiv:0704.3409 [hep-ph]]; A. Sabio Vera and F. Schwennsen, Nucl. Phys. B **776**, 170 (2007) [hep-ph/0702158 [hep-ph]].
5. A. H. Mueller and H. Navelet, Nucl. Phys. B **282**, 727 (1987); C. Marquet and C. Royon, Phys. Rev. D **79**, 034028 (2009) [arXiv:0704.3409 [hep-ph]]; A. Sabio Vera and F. Schwennsen, Nucl. Phys. B **776**, 170 (2007) [hep-ph/0702158 [hep-ph]]; B. Ducloué, L. Szymanowski and S. Wallon, Phys. Rev. Lett. **112**, 082003 (2014) [arXiv:1309.3229 [hep-ph]].
6. V. S. Fadin and L. N. Lipatov, Phys. Lett. B **429**, 127 (1998) [hep-ph/9802290 [hep-ph]]; M. Ciafaloni, Phys. Lett. B **429**, 363 (1998) [hep-ph/9801322 [hep-ph]]; M. Ciafaloni and G. Camici, Phys. Lett. B **430**, 349 (1998) [hep-ph/9803389 [hep-ph]].
7. G. P. Salam, JHEP **9807**, 019 (1998) [hep-ph/9806482 [hep-ph]].

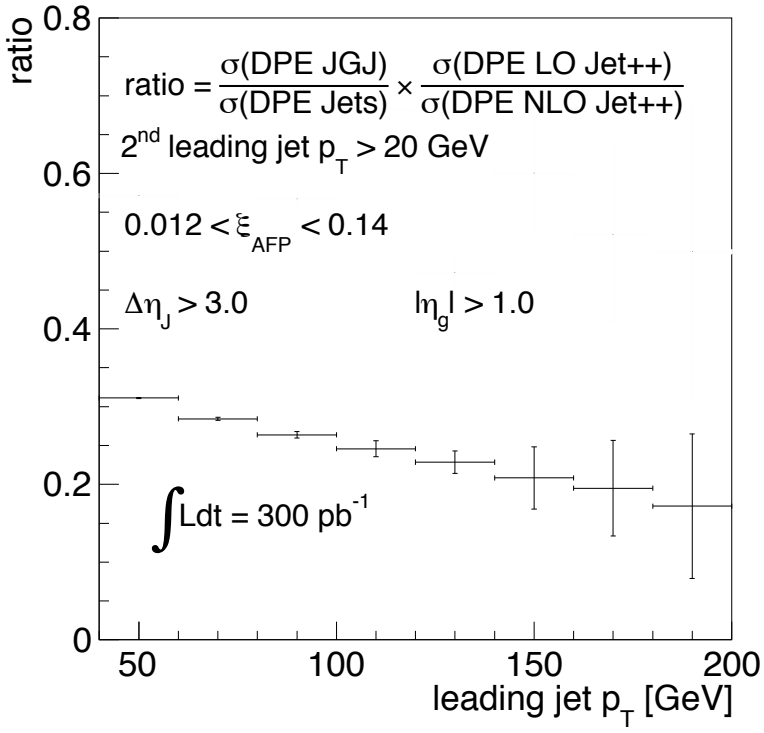

Figure 142: Ratio of the jet gap jet to the inclusive jet cross sections at the LHC as a function of jet p_T in double pomeron exchange events where the protons are detected in AFP.

8. A. Aktas *et al.* [H1 Collaboration], Eur. Phys. J. C **46**, 27 (2006) [hep-ex/0508055 [hep-ex]].
9. C. D. White, R. B. Peschanski and R. S. Thorne, Phys. Lett. B **639**, 652 (2006) [hep-ph/0606169 [hep-ph]].
10. G. Aad *et al.* [ATLAS Collaboration], JHEP **1109**, 053 (2011) [arXiv:1107.1641 [hep-ex]].
11. Y. Hatta, C. Marquet, C. Royon, G. Soyez, T. Ueda and D. Werder, Phys. Rev. D **87**(5), 054016 (2013) [arXiv:1301.1910 [hep-ph]].
12. O. Kepka, C. Marquet and C. Royon, Phys. Rev. D **83**, 034036 (2011) [arXiv:1012.3849 [hep-ph]]; F. Chevallier, O. Kepka, C. Marquet and C. Royon, Phys. Rev. D **79**, 094019 (2009) [arXiv:0903.4598 [hep-ph]].
13. G. Marchesini, B. R. Webber, G. Abbiendi, I. G. Knowles, M. H. Seymour and L. Stanco, Comput. Phys. Commun. **67**, 465 (1992).
14. Z. Nagy and Z. Trocsanyi, Phys. Rev. Lett. **87**, 082001 (2001) [hep-ph/0104315 [hep-ph]].
15. B. Abbott *et al.* [D0 Collaboration], Phys. Lett. B **440**, 189 (1998) [hep-ex/9809016 [hep-ex]]; F. Abe *et al.* [CDF Collaboration], Phys. Rev. Lett. **80**, 1156 (1998).
16. . Marquet, C. Royon, M. Trzebiński and R. Žlebčík, Phys. Rev. D **87**(3), 034010 (2013) [arXiv:1212.2059 [hep-ph]].
17. ATLAS Collaboration, report CERN-LHCC-2011-012.
18. C. Marquet, C. Royon, M. Saimpert and D. Werder, Phys. Rev. D **88**(7), 074029 (2013) [arXiv:1306.4901 [hep-ph]]; S. Fichet, G. von Gersdorff, O. Kepka, B. Lenzi, C. Royon and M. Saimpert, Phys. Rev. D **89**, 114004 (2014) [arXiv:1312.5153 [hep-ph]]; E. Chapon, C. Royon and O. Kepka, Phys. Rev. D **81**, 074003 (2010) [arXiv:0912.5161 [hep-ph]]; O. Kepka and C. Royon, Phys. Rev. D **78**, 073005 (2008) [arXiv:0808.0322 [hep-ph]]; S. Fichet, G. von Gersdorff, B. Lenzi, C. Royon and M. Saimpert, JHEP **1502**, 165 (2015) [arXiv:1411.6629 [hep-ph]].